JOURNAL OF MATERIALS SCIENCE 13(1978) 2577–2586

The influence of surface structures on sputtering: Angular distribution and yield from faceted surfaces

UFFE LITTMARK
H. C. Ørsted Institute, University of Copenhagen, DK-2100 Copenhagen, Denmark
WOLFGANG O. HOFER
Max-Planck-Institut für Plasmaphysik, D-8046 Garching bei München, Germany*

Solid surfaces subject to energetic particle bombardment generally develop characteristic structures, which may significantly change the total and differential sputtering yield. The change is due to two competing effects, a yield-increase by an enhanced effective projectile incidence angle, and a yield-reduction by recapture of obliquely ejected particles. Both effects have been included in calculations of the sputtering yields from faceted surfaces in the regime where the plane surface yield follows a $\cos^{-\nu}$ dependence on the incidence angle. Except at very low energies, the total sputtering yield is always increased by faceting. The angular distribution function is mainly influenced at large polar angles and may significantly deviate from that of the corresponding flat surface. This has important consequences both in comparisons between experimental and theoretical distribution functions as well as in applications such as thin film production, plasma contamination, secondary ion mass spectrometry etc.

1. Introduction

Surfaces of solids subject to energetic particle irradiation, in general show characteristic structures such as cones [1–4], facets [5–10], ridges [7–10], pyramids [7–9], amphitheatres [10], mushrooms [11], etc. These surface topographical effects are particularly pronounced on polycrystalline and/or multicomponent samples [12], but most of the characteristic features are apparent also on elemental single crystal surfaces. Only a few systems are known to remain flat under particle irradiation: solids which become amorphous during inert gas bombardment, such as most of the semiconductors [13], and solids whose lattice influence on the energy dissipation is destroyed by the presence of reactive gas in the surface layers [3].

It is now well established that both cones and facets can be generated irrespective of the presence of impurities or grain boundaries [4, 14]. One should thus clearly distinguish between heterogeneous systems which by definition contain structural discontinuities and therefore local change in sputtering yield, and "pure" systems, where accumulations of, and stresses around dislocations similarly cause alteration in sputtering yield. These two different effects provide the origins for the development of surface topographies. It is, however, not the purpose of this contribution to deal with these mechanisms, but to illuminate some of the consequences of deviations from a flat surface. Owing to a larger effective incidence angle of the projectiles on structured surfaces and due to recapture of ejected target particles by cones, ridges etc. one may speculate which of these two competing effects may prevail. The sputtering yield may then be either higher or lower than that from flat surfaces.

*EURATOM Association.

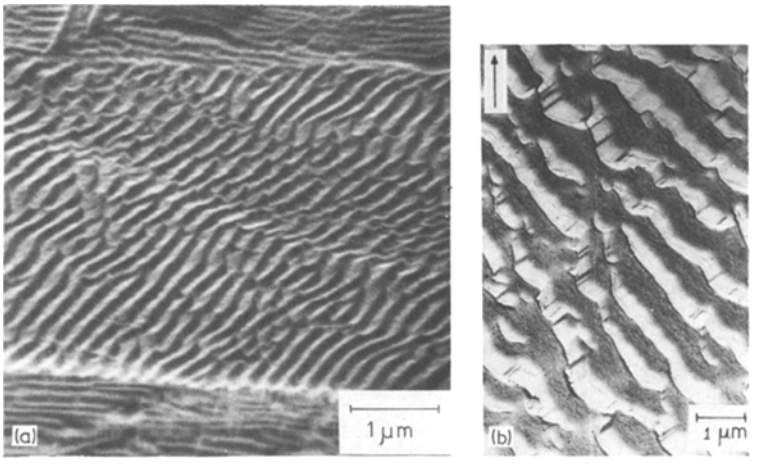

Figure 1 Typical facet structures obtained at very different irradiation and target conditions. (a) Scanning electron micrograph of polycrystalline Inconel bombarded with 4 keV helium ions. From H. L. Bay and J. Bohdansky, private communication. (b) Replica micrograph of a (1 0 0) copper single crystal bombarded with 20 keV neon ions. From J. J. Ph. Elich *et al.* [10].

Furthermore, the angular distribution of sputtered particles may be changed by the topography as well. This is of particular importance when emission distributions obtained from non-amorphous targets are used for comparison with theoretical results, as usually has been done in the past.

For practical applications it is mainly the total yield that is of importance since it determines both erosion speed and impurity load to the environment (e.g. plasma contamination due to sputtered wall atoms). In extreme cases, however, changes in the angular distribution can also be of significance, e.g. in sputter production of thin layers, where uniform deposition is required over large areas on the substrate. This is in particular a serious problem with multi-component layers, where cone formation on the sputter targets reduces the spatial and compositional homogeneity [12].

Apart from some aforementioned curiosities, surface structures are either of cone- or of facet-type nature. Only the latter structures are considered here. Their general appearance can be characterized as:

(i) often having perfect periodicity with well-defined facet angles and height, Fig. 1;

(ii) being rather sensitive to the incidence angle of the ion beam with respect to the lattice; and

(iii) showing correlation to the dislocation network.

These characteristics allow a rather general treatment of the yield problem of faceted surfaces – even more general than presented below, since we restrict ourselves to *those surface structures which are stable under the chosen irradiation conditions.* This restriction is not only for ease of presentation (or readability) but also for practical reasons. If a given structure is not stable under the chosen bombardment conditions*, it will change during the yield measurement, since the required fluence is of the order of 10^{17} to 10^{18} ions per cm^2. This constitutes a non-negligible fraction of the fluence necessary for establishing the corresponding stable structure, thus rendering the result obtained characteristic of neither the original nor the final structure. It would require rather sensitive techniques to investigate these transient effects. Although this is, in principle, possible, interest in this regime is limited.

For these reasons attention has been directed to the stationary problem in the sense that the facet angles remain unaltered during bombardment, i.e., the *type* of structure must be preserved. The *individual* facet may of course move across the surface.

2. Calculations

Let the faceted surface be characterized by the facet planes A and B, which are inclined at the angles α and β to the nominal (macroscopic) surface plane of the crystal. On each of these three planes a polar coordinate system is erected, the surface normals serving as polar axes and the plane of symmetry of the facets as the azimuthal reference plane, Fig. 2. All quantities referring to the facets A or B are identified by the respective

* This is generally the case when the bombardment conditions (energy, direction of incidence, projectile) are changed on the same target, but also for thermally or chemically faceted surfaces subjected to sputtering bombardment.

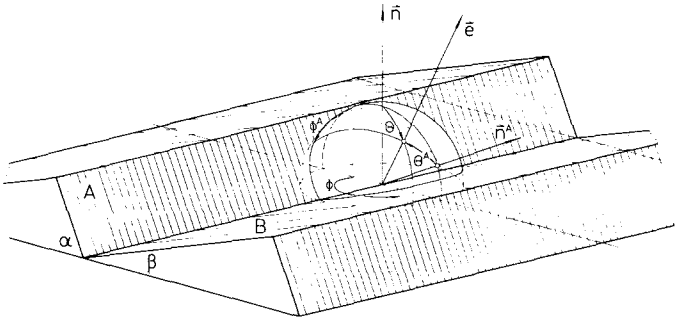

Figure 2 Definition of structure parameters, coordinate systems and reference planes.

superscripts, while quantities connected to the nominal surface have no index.

The transition relations between the systems are trivial; for instance the cosines of the polar angles, auxiliary quantities entering our final results, are

$$\begin{aligned} \cos\theta^{A} &= \cos\theta\cos\alpha - \sin\theta\sin\alpha\cos\phi \\ \cos\theta^{B} &= \cos\theta\cos\beta + \sin\theta\sin\beta\cos\phi \end{aligned} \tag{1}$$

Recapture of sputtered particles by the neighbouring facet plane will be treated as a shadowing effect (unit sticking probability assumed). For the description of this effect of the facets on the sputtered particles flux (the recapture) the two dimensional picture, Fig. 3, arising from the projection of Fig. 2 on the symmetry plane for the facets, is convenient. Directions are here specified by their angle ϵ to the nominal surface normal (measured clockwise). ϵ is connected to the polar coordinates by

$$\begin{aligned} \tan(\alpha-\epsilon) &= \tan\theta^{A}\cos\phi^{A} \\ &= \frac{\cos\theta\sin\alpha + \sin\theta\cos\alpha\cos\phi}{\cos\theta\cos\alpha - \sin\theta\sin\alpha\cos\phi} \\ \tan(\beta+\epsilon) &= \tan\theta^{B}\cos\phi^{B} \\ &= \frac{\cos\theta\sin\beta - \sin\theta\cos\beta\cos\phi}{\cos\theta\cos\beta + \sin\theta\sin\beta\cos\phi} \end{aligned} \tag{2}$$

All quantities and symbols pertinent to the incoming beam are characterized by subscript i, while quantities referring to the flux of sputtered (outgoing) particles by subscript o. Thus $\bar{e}_o$ is the direction of observation and $-\bar{e}_i$ the direction of bombardment. The directional region where sputtered material from part of plane A is shadowed by plane B is now

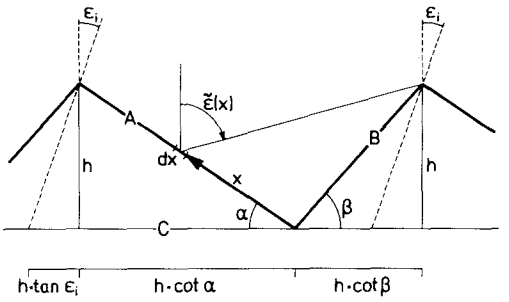

Figure 3 Characterization of the variables ϵ and x, shadowing limit $\tilde{\epsilon}(x)$ and beam partition.

$$\epsilon_o > \frac{\pi}{2} - \beta \quad \text{or}$$

$$-1 < \cos\phi_o < -\cot\beta\cot\theta_o \quad \text{(case I)} \tag{3}$$

and vice versa

$$\epsilon_o < \alpha - \frac{\pi}{2} \quad \text{or}$$

$$\cot\alpha\cot\theta_o < \cos\phi_o < 1 \quad \text{(case III)} \tag{4}$$

In all remaining directions

$$\alpha - \frac{\pi}{2} < \epsilon_o < \frac{\pi}{2} - \beta \quad \text{or}$$

$$-\cot\beta\cot\theta_o < \cos\phi_o < \cot\alpha\cot\theta_o$$

$$\text{(case II)} \tag{5}$$

no shadowing effects occur.

A similar distinction could be made for the incoming beam, but it has been omitted here because a situation where the facets shield the incoming beam is unstable, and so explicitly excluded from consideration.

The differential sputtering yield $dS(\bar{e}_i, \bar{e}_o)/d\Omega_o$ is the number of particles emitted per solid angle

element $d\Omega_o$ around e_o per projectile impinging on the surface from direction $\bar{e}_i$. Provided that the shape of the emission distribution for a flat surface is not dependent on the direction of projectile incidence*, the differential yield from a flat surface can be written

$$dS(\bar{e}_i, \bar{e}_o) \equiv f_i(\bar{e}_i) f_o(\bar{e}_o) d\Omega_o$$
$$= f_i(\cos\theta_i) f_o(\cos\theta_o) d\Omega_o \quad (6)$$

where in the second line the further assumption has been made that there exist no azimuthal dependences. This is a fair approach even for single crystals since random emission always dominates anisotropic effects [15, 16]. Preferential ejection from single crystals amounts to 20 to 30% of the total ejection and is observable only owing to its sharp distribution function. It is of minor importance for the total amount of ejected material, and particularly in case of polycrystalline targets.

The problem of sputtering from a faceted surface can now be treated as the superposition of sputtering from the A and B planes separately, taking into account the shadowing effects, but assuming that the facet planes are so large that edge effects can be neglected.

A particle sputtered from a point on plane A, a distance x above the facet bottom (see Fig. 3), has to satisfy

$$\epsilon_0 \in \left[\alpha - \frac{\pi}{2}, \tilde{\epsilon}(x)\right] \quad (7)$$

not to be recaptured; $\tilde{\epsilon}$ is the value of ϵ corresponding to the direction from the sputtering point to the B-plane top.

If N^A projectiles hit A it is easily verified that the number of projectiles hitting the element dx at x is

$$dN^A = N^A \frac{\sin\alpha}{h} dx$$
$$= N^A \frac{\sin\alpha \sin(\alpha+\beta)}{\sin\beta} d\tan(\tilde{\epsilon} - \alpha) \quad (8)$$

where h is the facet height. Thus the yield from A is found by integrating over $\tilde{\epsilon}$

$$\frac{dS^A}{d\Omega_o} = \frac{1}{N^A} \int f_i f_o dN^A$$
$$= \frac{\sin\alpha \sin(\alpha+\beta)}{\sin\beta} f_i f_o \tan(\tilde{\epsilon} - \alpha) \Big|_{\tilde{\epsilon}=M}^{\pi/2} \quad (9)$$

where $M = \max\{\pi/2 - \beta, \epsilon_o\}$.

From Equation 2 we obtain the relation

$$\cot\alpha + \tan(\alpha - \epsilon)$$
$$= \frac{1}{\sin^2\alpha} \frac{1}{\cot\alpha + \tan\epsilon} = \frac{1}{\sin\alpha} \frac{\cos\theta}{\cos\theta^A} \quad (10)$$

which inserted in Equation 9 yields

$$\frac{dS^A}{d\Omega_o} = f_i(\cos\theta_i^A) f_o(\cos\theta_o^A)$$
$$\times \begin{cases} 1 \text{ for } \cos\phi_o < -\cot\theta_o \cot\beta \\ \dfrac{\sin(\alpha+\beta)}{\sin\beta} \dfrac{\cos\theta_o}{\cos\theta_o^A} \text{ for } \cos\phi_o > -\cot\theta_o \cot\beta \end{cases} \quad (11)$$

Similarly the yield from the B-plane can be determined:

$$\frac{dS^B}{d\Omega_o} = f_i(\cos\theta_i^B) f_o(\cos\theta_o^B)$$
$$\times \begin{cases} 1 \text{ for } \cos\phi_o < \cot\theta_o \cot\alpha \\ \dfrac{\sin(\alpha+\beta)}{\sin\alpha} \dfrac{\cos\theta_o}{\cos\theta_o^B} \text{ for } \cos\phi_o > \cot\theta_o \cot\alpha \end{cases} \quad (12)$$

The differential sputtering yield from the faceted surface is now obtained by linear superposition of the weighted ejection intensities Equations 11 and 12:

$$\frac{dS^{A+B}}{d\Omega_o} = 1/N \left(N^A \frac{dS^A}{d\Omega_o} + N^B \frac{dS^B}{d\Omega_o} \right) \quad (13)$$

where

$$N^A = N \frac{\cot\alpha + \tan\epsilon_i}{\cot\alpha + \cot\beta} = N \frac{\sin\beta}{\sin(\alpha+\beta)} \frac{\cos\theta_i^A}{\cos\theta_i} \quad (14)$$

and

$$N^B = N \frac{\sin\alpha}{\sin(\alpha+\beta)} \frac{\cos\theta_i^B}{\cos\theta_i} \quad (15)$$

are found by use of Fig. 3 and Equation 10.

* This is essentially a limit towards low energies, where a "specular component" in the emission distribution might be present [17–20].

From Equation 13 the total yield S is obtained by integration over the whole free space of emission ($\alpha - \pi/2 < \epsilon_o < \pi/2 - \beta$). The specific form of $f_o(\cos\theta_o)$ has to be introduced at this point. The integration is most easily performed in a polar system having the facet edge as the axis and therefore ϵ_o as azimuthal angle.

3. Results and discussion

Inserting the results from Equations 11, 12, 14 and 15 in Equation 13, the differential yield from the faceted surface is found to be

$$\frac{dS^{A+B}}{d\Omega_o} = \begin{cases} f_i(\cos\theta_i^A)\dfrac{\cos\theta_i^A}{\cos\theta_i} f_o(\cos\theta_o^A)\dfrac{\cos\theta_o}{\cos\theta_o^A} & \text{case I,} \\ f_i(\cos\theta_i^A)\dfrac{\cos\theta_i^A}{\cos\theta_i} f_o(\cos\theta_o^A)\dfrac{\sin\beta}{\sin(\alpha+\beta)} + & \\ \quad f_i(\cos\theta_i^B)\dfrac{\cos\theta_i^B}{\cos\theta_i} f_o(\cos\theta_o^B)\dfrac{\sin\alpha}{\sin(\alpha+\beta)} & \text{case II, and} \\ f_i(\cos\theta_i^B)\dfrac{\cos\theta_i^B}{\cos\theta_i} f_o(\cos\theta_o^B)\dfrac{\cos\theta_o}{\cos\theta_0^B} & \text{case III.} \end{cases} \quad (16)$$

The above mentioned integration of Equation 16 to obtain the total yield can easily be performed using the power form

$$f_o(\cos\theta_o) = (\cos\theta_o)^{\nu_o} \quad (17)$$

Any emission distribution f_o, which is rotationally symmetric around the nominal surface normal can be described by a polynomial in $\cos\theta_o$. In many cases $\nu_o = 1, 2$ will be sufficient: one may construct "undercosine" as well as "overcosine" distributions from just these two terms. Furthermore $\nu_o = 1$ is the value predicted from random collision cascade theory (in the isotropic approach), thus most considerations are devoted to this case.

For $\nu_o = 1$ the integration of Equation 16 yields

$$S^{A+B} = \frac{\pi}{2}\frac{\cos\theta_i^A}{\cos\theta_i} f_i(\cos\theta_i^A)\left(1 - \frac{\sin\alpha - \sin\beta}{\sin(\alpha+\beta)}\right) + \frac{\pi}{2}\frac{\cos\theta_i^B}{\cos\theta_i} f_i(\cos\theta_i^B)\left(1 - \frac{\sin\beta - \sin\alpha}{\sin(\alpha+\beta)}\right) \quad (18)$$

whereas $\nu_o = 2$ results in

$$S^{A+B} = \frac{2}{3}\frac{\cos\theta_i^A}{\cos\theta_i} f_i(\cos\theta_i^A) \times [(\pi-\alpha)\cos\alpha - (\pi-\alpha-\beta)\sin\alpha\cot(\alpha+\beta)] + \frac{2}{3}\frac{\cos\theta_i^B}{\cos\theta_i} f_i(\cos\theta_i^B) \times [(\pi-\beta)\cos\beta - (\pi-\alpha-\beta)\sin\beta\cot(\alpha+\beta)] \quad (19)$$

The results so far obtained are valid for all types of $f_i(\cos\theta_i)$ distributions. For a more specific discussion, with special attention to the problem of increase/decrease of the total yield relative to the yield from the flat nominal surface, we now pay attention only to the ascending branch of $f_i(\cos\theta_i)$. This means that reflection of projectiles and thereby enhanced sputtering from the facet-bottom is neglected. Under these conditions

$$f_i(\cos\theta_i) = A_i(\cos\theta_i)^{\nu_i}, \quad \nu_i < 0 \quad (20)$$

applies quite generally. A_i is a constant depending on energy and the type of ion and target. Inclusion of the descending branch of f_i would not introduce any severe complications in the calculations [21], but the physical model becomes doubtful in this regime of incidence angles. The applicability of the following relations based on Equation 20 is therefore limited to $\theta_i^A, \theta_i^B \lesssim 70°$.

The differential yield in Equation 16, relative to the corresponding yield for the nominal surface, is then with Equation 20

$$\frac{dS^{A+B}/d\Omega_o}{dS/d\Omega_o} = \begin{cases} \left(\frac{\cos\theta_i^A}{\cos\theta_i}\right)^{\nu_i+1}\left(\frac{\cos\theta_o^A}{\cos\theta_o}\right)^{\nu_o-1} & \text{case I,} \\ \left(\frac{\cos\theta_i^A}{\cos\theta_i}\right)^{\nu_i+1}\left(\frac{\cos\theta_o^A}{\cos\theta_o}\right)^{\nu_o}\frac{\sin\beta}{\sin(\alpha+\beta)} + & \\ \quad \left(\frac{\cos\theta_i^B}{\cos\theta_i}\right)^{\nu_i+1}\left(\frac{\cos\theta_o^B}{\cos\theta_o}\right)^{\nu_o}\frac{\sin\alpha}{\sin(\alpha+\beta)} & \text{case II,} \\ \left(\frac{\cos\theta_i^B}{\cos\theta_i}\right)^{\nu_i+1}\left(\frac{\cos\theta_o^B}{\cos\theta_o}\right)^{\nu_o-1} & \text{case III.} \end{cases} \quad (21)$$

and the relative total yield is

$$\frac{S^{A+B}}{S} = \frac{1}{2}\left(\frac{\cos\theta_i^A}{\cos\theta_i}\right)^{\nu_i+1}\left(1-\frac{\sin\alpha-\sin\beta}{\sin(\alpha+\beta)}\right) + \frac{1}{2}\left(\frac{\cos\theta_i^B}{\cos\theta_i}\right)^{\nu_i+1}\left(1-\frac{\sin\beta-\sin\alpha}{\sin(\alpha+\beta)}\right) \quad (22)$$

for $\nu_o = 1$, and

$$\frac{S^{A+B}}{S} = 1/\pi\left(\frac{\cos\theta_i^A}{\cos\theta_i}\right)^{\nu_i+1} \times [(\pi-\alpha)\cos\alpha - (\pi-\alpha-\beta)\sin\alpha\cot(\alpha+\beta)] + 1/\pi\left(\frac{\cos\theta_i^B}{\cos\theta_i}\right)^{\nu_i+1} \times [(\pi-\beta)\cos\beta - (\pi-\alpha-\beta)\sin\beta\cot(\alpha+\beta)] \quad (23)$$

for $\nu_o = 2$.

Before presenting numerical examples a few special aspects of these formulae are discussed:

(i) For $\nu_i = -1$ $(f_i = A_i\cos^{-1}\theta_i)$,

$\frac{dS^{A+B}}{d\Omega_o}$ is independent of the aximuth ϕ_i,

$\frac{dS^{A+B}/d\Omega_o}{dS/d\Omega_o}$ is independent of the direction of bombardment $\bar{e}_i$ and S^{A+B}/S is a constant, only depending on the facet angles α and β. These results are valid whatever the emission distribution is. If further

(ii) $\nu_i = -1$ and $\nu_o = 1$ $(f_o = \cos\theta_o)$

$\frac{dS^{A+B}}{d\Omega_o}$ is independent of both ϕ_o and ϕ_i and

$\frac{dS^{A+B}/d\Omega_o}{dS/d\Omega_o} = 1$ and $S^{A+B}/S = 1$.

This means that *both the angular distribution and the total yield from the faceted surface are indistinguishable from those of a flat surface.* Neither the facet angles nor the impact angle have any influence on the relative yields.

While $\nu_i = -1$ is in general not well verified experimentally,

(iii) $\nu_o = 1$ gives a very good description for most of the experimental data at medium to high projectile energy. In this case Equation 22 gives

$$S^{A+B}/S \begin{cases} > 1 & \text{for } \nu_i < -1 \\ < 1 & \text{for } \nu_i > -1 \end{cases} \quad (24)$$

This result is remarkable since it quite generally shows that, owing to ν_i usually being between -1 and -2, faceted surfaces show higher sputtering yields than flat surfaces. Thus the increase in yield caused by the enhanced effective projectile incidence angle is stronger than the reduction due to shadowing. There are only few experimental investigations where the sputtering yield has been measured for well-characterized surface structures [20–24] but the general observation is in good agreement with the above result.

Special features are found for

(iv) $\phi_i = \pi/2$, $\phi_i = 3\pi/2$, i.e. when the projection of the beam direction on the nominal surface coincides with the line of intersection of the facet planes. Then

$\frac{dS^{A+B}/d\Omega_o}{dS/d\Omega_o}$ and S^{A+B}/S are independent of θ_i.

Similarly for

(v) $\phi_o = \pi/2$, $\phi_o = 3\pi/2$, i.e. when the projection of the direction of observation on the nominal surface coincides with the line of intersection of the facet planes,

$\frac{dS^{A+B}/d\Omega_o}{dS/d\Omega_o}$ is independent of θ_o.

So in these emission directions the facets do not create any distortion in the shape of the emission distribution.

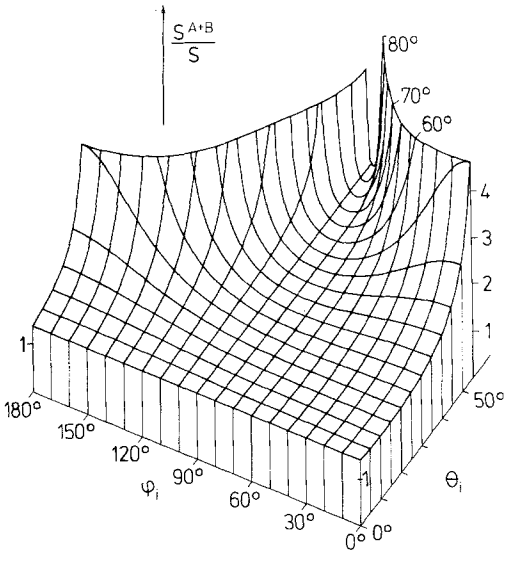

Figure 4 Relative total sputtering yields for a faceted surface with facet angles $\alpha = 30°, \beta = 60°, f_i = A_i \cos^{-2} \theta_i$, $f_o = \cos \theta_o$.

The Relations 16, 21, 22 and 23 have been examined in more detail for the specific choice of $\alpha = 30°$, $\beta = 60°$. While $\nu_o = 1$, $\nu_i = -1$ yields $S^{A+B}/S = 1$ (Equation 22), $\nu_o = 2$, $\nu_i = -1$ gives $S^{A+B}/S = 1.055$ (Equation 23); so for $\nu_i = -1$ the shape of the emission distribution has only a minor influence. The same result is obtained for $\nu_i = -2$, but here the direction of incidence influences S^{A+B}/S drastically. Fig. 4 shows this particular case. The curves have been drawn up to 5° from grazing incidence on the facet planes, primarily to illustrate the tendency. Only values up to ~ 20° from grazing incidence are realistic. The main observation from Fig. 4 is, as mentioned above, that *the yield from the faceted surface always exceeds the yield from a flat surface.*

From purely qualitative arguments we infer this behaviour to hold true also for pyramid-type structures. The yield-enhancement owing to increased effective ion incident angle remains unchanged but the probability of released particles escaping recapture is enhanced; for a regular array of pyramids this is rather obvious, while for an irregular array statistical arguments can be put forward. Having accepted this argument, there is no reason why one should not reach the same conclusion for structures of circular cross-sections, i.e. "proper" cones. Only when projectiles get reflected from the faces of the structure towards the deeper – hence well shielded – regions, is yield reduction by surface topography expected. Under these grazing incidence conditions not only does the major part of the released particles get recaptured; also the effective incidence angle becomes nearer to perpendicular. This is the typical case of yield reduction by cones with small opening angles (needle-like cones), a situation which is well beyond the applicability regime of Equations 21 to 23. It is to be noted that this effect has often incorrectly been generalized for rough surfaces, while it only applies for extremely large impact angles*.

There are not too many experimental investigations of the yield for well-defined surface structures. Elich *et al.* [10] have performed extensive measurements on Cu single crystals and found an increase for facet structures like that shown in Fig. 2. Rödelsperger and Scharmann [20] reported enhanced differential yields for 130 keV to 1 MeV Ar^+ ions on several polycrystalline targets with pronounced structure. Roth *et al.* [23] found higher yields on stainless steel bombarded with 2 keV H^+ when the surface was heavily structured. Blank and Wittmaack [24, 25] explained their significantly lower yields of Si in terms of smoother surfaces as compared to Andersen and Bay [26]. The opposite case, yield reduction by surface topography, has been observed without exception for grazing incidence only. Although this applies for a rather small interval of impact angles, $70° \leqslant \theta^{A,B} \leqslant 90°$, the situation can often be met for impurity induced structures, because their protective tips lead to needle- or pillar-like configurations.

In Figs. 5a to e emission distributions are shown in polar plots. For fixed facet angles $\alpha = 30°$ and $\beta = 60°$ Equation 16 was evaluated at two different ion incidence directions, $(0°, 0°)$ and $(45°, 45°)$, as well as various distribution functions f_i, f_o. The heavy full drawn curve is the emission distribution from the flat surface; it coincides with the (normalized) emission distribution obtained at an azimuth of $\phi_o = 90°$. This special case, together with the above discussed result for $\nu_i = -1$, $\nu_o = 1$, shows no distortion of the emission distribution for a flat surface. All the other cases show substantial deviations due to the influence of the topography. This is particularly obvious when one measures at the $\phi_o = 0$, 180° azimuth, where kinks in the distribution function indicate the onset of shadowing towards

* With respect to the micro-planes building up the structure.

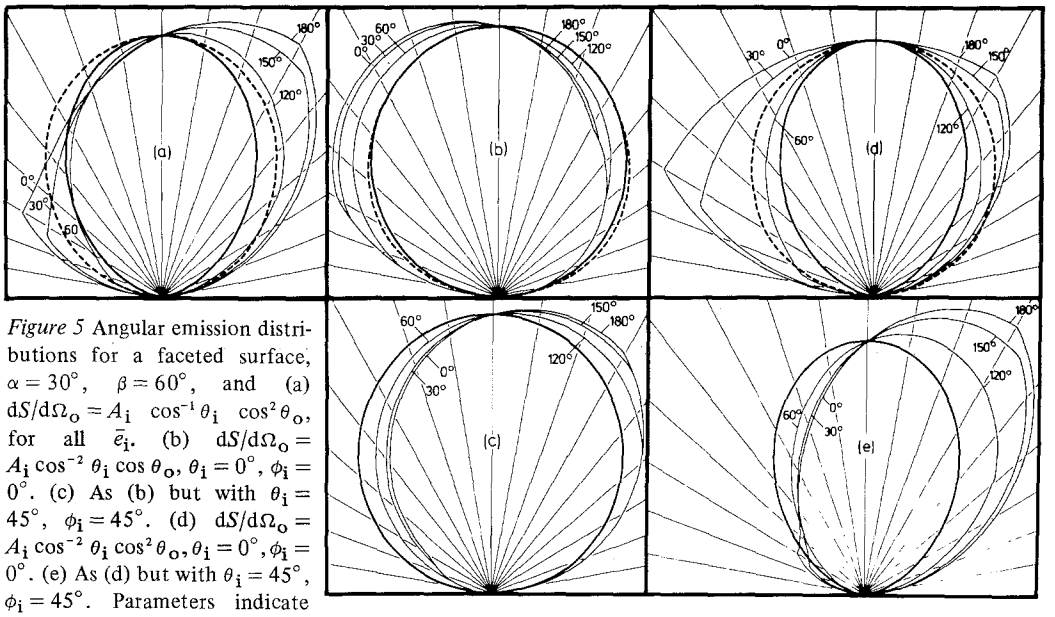

Figure 5 Angular emission distributions for a faceted surface, $\alpha = 30°$, $\beta = 60°$, and (a) $dS/d\Omega_o = A_i \cos^{-1}\theta_i \cos^2\theta_o$, for all $\bar{e}_i$. (b) $dS/d\Omega_o = A_i \cos^{-2}\theta_i \cos\theta_o$, $\theta_i = 0°$, $\phi_i = 0°$. (c) As (b) but with $\theta_i = 45°$, $\phi_i = 45°$. (d) $dS/d\Omega_o = A_i \cos^{-2}\theta_i \cos^2\theta_o$, $\theta_i = 0°$, $\phi_i = 0°$. (e) As (d) but with $\theta_i = 45°$, $\phi_i = 45°$. Parameters indicate the azimuthal angle ϕ_o. Heavy full-drawn curves are the flat surface yield coinciding with the $\phi_o = 90°$-distributions. Dashed curves are obtained by averaging over ϕ_o.

higher polar angles. While such extreme results can only be expected on single crystals, a polycrystalline situation is better described by distribution functions averaged over ϕ_o for fixed $\phi_i - \phi_o$, since here the random orientation of the different grains smears out the azimuthal information*.

The general impression transpiring from the ϕ_o-averaged, dashed curves, (here only shown for normal incidence) is their tendency to approach a cosine distribution, even though the genuine distribution may be of quite different character. The agreement with the results of random collision cascade theory and many experiments, although at first sight gratifying, may therefore be fortuitous. This emphasizes the need for a detailed surface characterization when measuring differential sputtering yields. For the comparison with theories it is especially important that emission distributions be obtained from structureless surfaces.

It is obvious from these results that the surface structure exerts a profound influence on the differential yield. This finding is in glaring contradiction to the calculations of Gurmin *et al.* [17], where even heavily structured ("louvered") surfaces were still shown to reflect the emission distribution from flat surfaces. This incorrect conclusion was reached because too special cases were generalized†. As previously mentioned, the case $\nu_i = -1$, $\nu_o = 1$ would lead to the same inferences, but this case can hardly be considered representative of the phenomenon as a whole.

The assumption of the topography having no influence on the differential yield [17] may have serious consequences. For instance, the determination of the total sputtering yield from the collected sputtered material requires an accurate measurement of the whole angular distribution for every set of experimental parameters [27]. This rules out the widely used flat collectors since with these collectors the uncertainty is largest where the increasing solid angle demands highest precision. The error is even worse if only selected deposit areas are registered; in this case the result would be in error even if a correct distribution function for the flat target surface were used. Another example where the strong deviations of the differential yield at high polar angles may cause erroneous conclusions, is the background subtraction procedure in sputtering spot-pattern evaluation [16]. A background-fit is generally

* Integrating over the azimuth ϕ_o implies the assumption that the same type of facet structure develops on the different grains. In view of Fig. 1a this seems to be a fair approach, but this does not necessarily apply for all targets.

† It is not clear from Gurmin *et al.*'s paper which type of f_i-dependence was considered; we presume $f_i \sim \cos^{-1}\theta_i$ has been chosen.

possible only at large polar angles, thus rendering this procedure again dependent on the detailed knowledge of the surface topography and its influence on the differential yield.

4. Conclusions

Surface structures developing under energetic particle irradiation have a strong influence on both the total and the differential yield. This is a consequence of the two counteracting effects; yield enhancement due to an enhanced effective projectile incidence angle, and recapture of ejected target particles by protruding elements of the structure. Both quantities have been included in calculations for regularly faceted surfaces under impact conditions where projectile reflection from facet planes can be neglected. This applies for the ascending branch of the yield versus incidence angle curve, which in general, extends from zero to about 70°.

The *differential yield* from flat surfaces was found to be strongly distorted by surface structures, particularly at grazing ejection angles. Extreme care has therefore to be exercised when angular emission distributions measured on polycrystals are interpreted in terms of cascade or momentum transfer mechanisms. In addition, the distortion at high polar angles renders the widely used flat collectors unsuitable for both differential and total yield measurements. There is, on the other hand, a surprisingly general class of experimental conditions, where faceting does not alter the angular emission distribution at all. This is especially true if the θ_o and θ_i dependence of the flat surface yield follows a cosine and inverse cosine law respectively; in this case neither by measuring the total nor the differential yield can the faceted surface be distinguished from the atomically flat one. The general tendency of facets, however, is to enhance emission at larger polar angles.

The *total yield* was found to be always enhanced by surface structures – except for the above mentioned $\nu_o = |\nu_i| = 1$ case, and at projectile energies near the sputtering threshold, where extreme under-cosine emission distributions are found, which then may lead to comparatively large recapture fractions. Under sputtering conditions determined by random collision cascades, however, the true emission distribution is very close to a cosine function and yield enhancement always prevails.

In view of these results it is concluded quite generally that yield reduction in collision cascade controlled sputtering only occurs when projectile reflection at steep slopes of the structure causes flux enhancement at the bottom of the structure, from where the escape probability is lowest.

Acknowledgements

It is our pleasure to thank H. L. Bay and J. L. Whitton for fruitful discussions and stimulating criticism.

References

1. A. GÜNTHERSCHULZE and W. TOLLMIEN, *Z. Physik* **119** (1942) 685.
2. G. K. WEHNER and D. J. HAJICEK, *J. Appl. Phys.* **42** (1971) 1145.
3. W. O. HOFER and H. LIEBL, *Appl. Phys.* 8 (1975) 359.
4. J. L. WHITTON, G. CARTER, M. J. NOBES and J. S. WILLIAMS, *Rad. Effects* **32** (1977) 129.
5. R. L. CUNNINGHAM and J. NG-YELIM, *J. Appl. Phys.* **40** (1969) 2904.
6. A. D. G. STEWART and M. W. THOMPSON, *J. Mater. Sci.* 4 (1969) 56.
7. B. NAVINSEK, *Prog. Surface Sci.* 7 (1976) 49.
8. G. CARTER, J. S. COLLIGON and M. J. NOBES, *Rad. Effects* **31** (1977) 65.
9. I. A. TEODORESCU and F. VASILIU, *ibid.* **15** (1972) 101.
10. J. J. Ph. ELICH, H. E. ROOSENDAAL, H. H. KERSTEN, D. ONDERLINDEN and J. KISTEMAKER, *ibid.* 8 (1971) 1.
11. J. L. WHITTON, private communication (1977).
12. Proceedings of the 7th Vacuum Congress and the 3rd International Conference on Solid Surfaces, Vienna (1977) edited by R. Dobrozemsky, F. Rüdenaner, F. P. Viehböck and A. Breth.
13. I. H. WILSON, "Ion Surface Interaction, Sputtering and related Phenomena," edited by R. Behrisch, W. Heiland, W. Poschenrieder, P. Staib and H. Verbeek (Gordon and Breach, London, New York, Paris, 1973) p. 217.
14. N. HERMANNE, *ibid.* p. 207.
15. N. Th. OLSON and H. P. SMITH, *Phys. Rev.* **157** (1967) 241.
16. W. O. HOFER, as [13] p. 7.
17. B. M. GURMIN, Yu. A. RYZHOV and I. I. SHKARBAN, *Bull. Acad. Sci. USSR Phys. Ser. (USA)* **33** (1968) 752.
18. G. BETZ, R. DOBROZEMSKY and F. P. VIEHBÖCK, *Nederl. Tijdschr. v. Vacuumtechniek* 8 (1970) 203.
19. *Idem, Int. J. Mass Spectrom. Ion Phys.* 6 (1971) 451.
20. K. RÖDELSPERGER and A. SCHARMANN, *Nucl. Instrum. Meth.* **132** (1976) 355.

21. J. P. DUCOMMUN, M. CANTAGREL and M. MARCHAL, *J. Mater. Sci.* **9** (1974) 725.
22. J. P. DUCOMMUN, M. CANTAGREL and M. MOULIN, *ibid.* **10** (1975) 52.
23. J. ROTH, J. BOHDANSKI, W. O. HOFER and J. KIRSCHNER, Proceedings of the International Symposium on Plasma Wall Interaction, Jülich, 1977 (Pergamon Press, Oxford, 1977) p. 309.
24. P. BLANK and K. WITTMAACK, *Verhandlg. Dt. Phys. Ges.* **12** (1977) 327.
25. P. BLANK, Thesis Universität München (1977).
26. H. H. ANDERSEN and H. L. BAY, *J. Appl. Phys.* **46** (1975) 1919.
27. H. L. BAY, J. BOHDANSKY, W. O. HOFER and U. LITTMARK, to be published.

Received 8 February and accepted 24 April 1978.